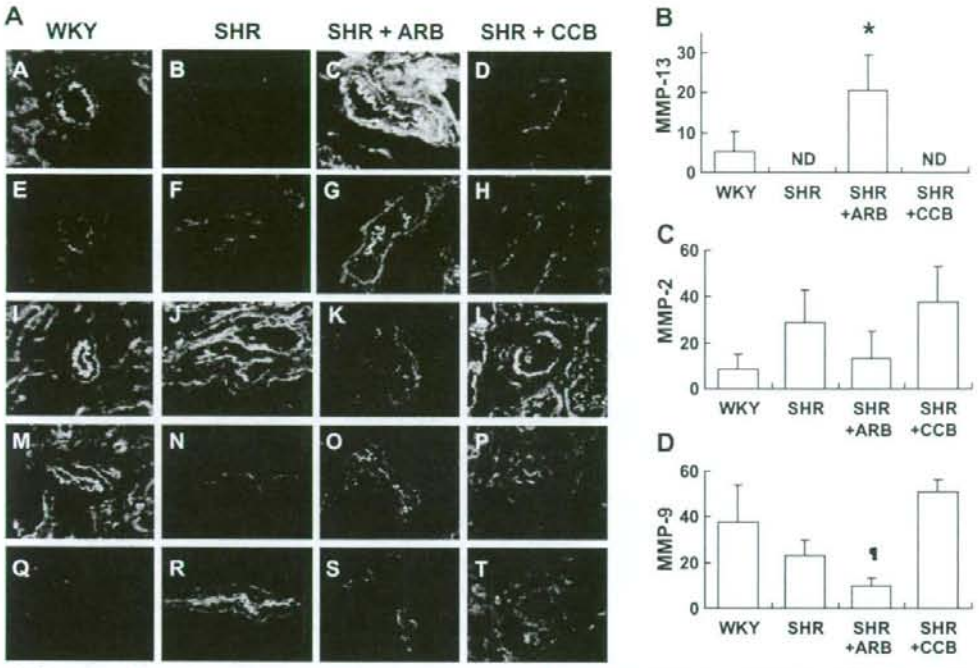

Figure 4. Short-term effects of pulse treatment with ARB or CCB on vascular MMP-13, MMP-2, and MMP-9 activities at age 18 weeks in SHRs. A, Representative in situ zymograms of (A through D) total type I collagenolytic activity; (E through H) type I collagenolytic activity in the presence of MMP-13 inhibitor; (I through L) total type IV collagenolytic activity; (M through P) type IV collagenolytic activity in the presence of MMP-2 inhibitor; and (Q through T) type IV collagenolytic activity in the presence of MMP-9 inhibitor. B through D, Quantification of (B) MMP-13, (C) MMP-2, and (D) MMP-9 activities in medial layers of renal arterioles. Abbreviations of groups as in Figure 2. *$P<0.05$ vs WKY rats; ¶$P<0.05$ vs SHR+CCB.

pulse treatment with different doses of ARB (1 to 50 mg/kg per day) on regression of glomerular hypertrophy and sclerosis and have found that the maximal effect on the regression of glomerular changes is obtained with the high dose (50 mg/kg per day) used in this study (unpublished observation).

One caveat of this study concerns the limitations of the indirect measurement of blood pressure. As in our previous studies, we performed the blood pressure measurements of the different groups on the same day, with the same experienced investigator, after an initial period of training under

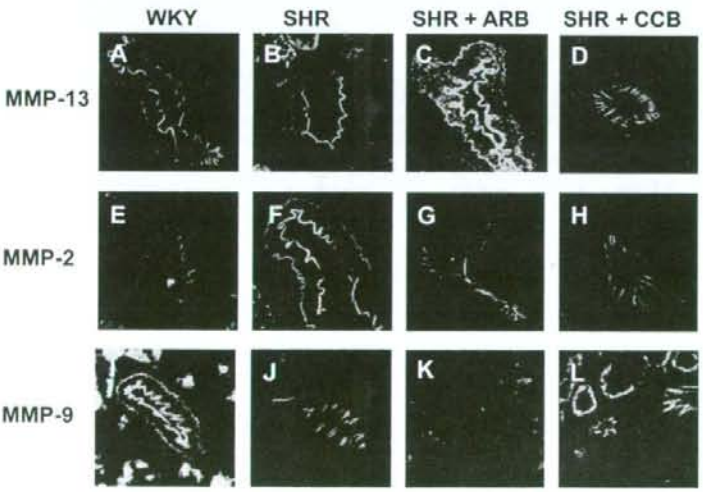

Figure 5. Short-term effects of pulse treatment with ARB or CCB on vascular MMP-13, MMP-2, and MMP-9 expression at age 18 weeks in SHRs. Immunofluorescent staining of (A through D) MMP-13 protein; (E through H) MMP-2 protein; and (I through L) MMP-9 protein.

stress-free conditions. Under these conditions, we found a clear-cut reduction of blood pressure (>30 to 40 mm Hg) in the ACEI- and ARB-treated groups every 2 weeks, consistently over several months, compared with the control, CCB-treated, and vasodilator-treated groups. However, it should be recognized that the indirect method is less accurate than direct measurement using an indwelling catheter, and absolute values of blood pressure may not be wholly reliable.[13] Moreover, unlike the telemetry method, the measurements were made at a single point and were not made continuously over multiple days; thus, small differences in blood pressure between the different groups at age 18 weeks cannot be accurately assessed. Because of the limited precision of the tail-cuff method, we cannot conclude whether the effects of ARB at age 18 weeks are entirely independent of blood pressure.

An important finding was that treatment with a high dose of ARB alone was sufficient to cause a remarkable reversal of renal arteriolar hypertrophy in the course of just 2 weeks. The media:lumen ratios of the small renal arterioles in the ARB pulse-treated rats were decreased almost to the levels found in the normotensive WKY rat, whereas the CCB did not have a significant effect. Several lines of evidence suggest that hypertrophy of the small arterioles in the kidney plays a major role in the pathogenesis of hypertension in the SHR.[10,11,14] Therefore, the observed reversal of renal arteriolar hypertrophy is compatible with the regression of hypertension seen in the ARB-treated groups.

Because we found marked changes in the kidney after just 2 weeks of pulse treatment, we performed a comprehensive survey (microarray analysis) of the differences in gene expression in the kidney of ARB-treated and CCB-treated rats. Interestingly, the microarray analysis did not reveal a major change in components of the RAS, except for an increase in renin mRNA, which could be expected as a feedback response to RAS inhibition. In contrast, expression of several extracellular matrix–related proteins, in particular, MMPs and TIMPs, was differently affected by the 2 treatments, and these results were confirmed by RT-PCR analysis. We focused on these findings, because changes in the expression of these genes could be involved in the remodeling of the renal arterioles. To clarify the changes in the renal arterioles, we assayed tissue MMP activity using a recently developed high-resolution, high-sensitivity in situ zymography technique.[12] Using this method, we found that the ARB treatment had different effects on the vascular MMP system than the CCB treatment and caused an increase in vascular MMP-13 activity and a decrease in MMP-9 activity, which could explain the different effects on regression of renal arteriolar hypertrophy. These findings were confirmed immunohistologically, by immunofluorescence staining of these MMPs.

It is well established that the MMPs, in particular, members of the collagenase and gelatinase families, play an important role in tissue remodeling by cleaving many structural proteins of the extracellular matrix.[15] MMP-13 is the predominant collagenase in rodents that lack the gene for MMP-1 and is involved in the collagenolysis of types I, II, and III collagens.[16] MMP-13 is known to be expressed in cultured vascular smooth muscle cells[17] and has been implicated in remodeling of the uterine artery during pregnancy,[18] in angiogenesis,[19] and in aneurysm formation.[17] These reports are consistent with the notion that upregulation of vascular MMP-13 activity by high-dose ARB in this model will result in collagenolysis of vascular collagens, favoring regression of renal arteriolar hypertrophy. It has been reported that MMP-9 (gelatinase B) is also expressed in cultured vascular smooth muscle cells, where it is involved in cell migration[20] and is upregulated by angiotensin II.[21] Therefore, the inhibition of MMP-9 by ARB could cause inhibition of compensatory smooth muscle cell migration, further contributing to the vascular changes.

The results of this study extend the work of Smallegange et al[9] using ACEI and a low-salt diet. In their studies, they found that cross-transplantation of kidneys from rats treated transiently with ACEI and a low-salt diet to hypertensive rats caused a transfer of the sustained reduction of blood pressure, whereas the untreated kidneys caused an increase in blood pressure. Moreover, the ACEI and low-salt treatment caused a significant decrease in renal vascular resistance. We speculate that the marked regression of renal small arteriolar hypertrophy ("renal microvascular remodeling") reported in this study is intimately involved in the mechanism of hypertension regression found in these models.

Perspectives

Because the animal studies on the prevention of hypertension development were successfully confirmed clinically by the Trial of Preventing Hypertension,[8] we have now designed a multicenter prospective clinical study (Short Treatment With Angiotensin Receptor Candesartan Surveyed by Telemedicine Study) to examine the feasibility of regression of established hypertension (ie, reversal from stage 1 to prehypertension) using transient ARB treatment in patients with essential hypertension.[22] The results of this study lead us to speculate that the development of methods to cause regression (or cure) of hypertension, and the study of the mechanisms of regression, may become one of the central themes in hypertension research this century.

Acknowledgment

We are grateful to Dr Norman M. Kaplan, Southwestern Medical Center, for helpful discussion and comments about this article.

Sources of Funding

This work was supported by grants 20590984, 17590844, and 18790578 from the Ministry of Education, Culture, Science and Technology, Japan.

Disclosures

None.

References

1. Kearney PM, Whelton M, Reynolds K, Muntner P, Whelton PK, He J. Global burden of hypertension: analysis of worldwide data. *Lancet*. 2005; 365:217–223.
2. Lawes CM, Vander Hoorn S, Rodgers A. Global burden of blood-pressure-related disease, 2001. *Lancet*. 2008;371:1513–1518.
3. Harrap SB, Van der Merwe WM, Griffin SA, Macpherson F, Lever AF. Brief angiotensin converting enzyme inhibitor treatment in young spon-

taneously hypertensive rats reduces blood pressure long-term. *Hypertension*. 1990;16:603–614.
4. Richer C, Mulder P, Fornes P, Richard V, Camilleri JP, Giudicelli JF. Hemodynamic and morphological effects of quinapril during genetic hypertension development. *J Cardiovasc Pharmacol*. 1991;18:631–642.
5. Nakaya H, Sasamura H, Hayashi M, Saruta T. Temporary treatment of prepubescent rats with angiotensin inhibitors suppresses the development of hypertensive nephrosclerosis. *J Am Soc Nephrol*. 2001;12:659–666.
6. Nakaya H, Sasamura H, Mifune M, Shimizu-Hirota R, Kuroda M, Hayashi M, Saruta T. Prepubertal treatment with angiotensin receptor blocker causes partial attenuation of hypertension and renal damage in adult Dahl salt-sensitive rats. *Nephron*. 2002;91:710–718.
7. Ishiguro K, Sasamura H, Sakamaki Y, Itoh H, Saruta T. Developmental activity of the renin-angiotensin system during the "critical period" modulates later L-NAME-induced hypertension and renal injury. *Hypertens Res*. 2007;30:63–75.
8. Julius S, Nesbitt SD, Egan BM, Weber MA, Michelson EL, Kaciroti N, Black HR, Grimm RH Jr, Messerli FH, Oparil S, Schork MA. Feasibility of treating prehypertension with an angiotensin-receptor blocker. *N Engl J Med*. 2006;354:1685–1697.
9. Smallegange C, Hale TM, Bushfield TL, Adams MA. Persistent lowering of pressure by transplanting kidneys from adult spontaneously hypertensive rats treated with brief antihypertensive therapy. *Hypertension*. 2004;44:89–94.
10. Skov K, Mulvany MJ. Structure of renal afferent arterioles in the pathogenesis of hypertension. *Acta Physiol Scand*. 2004;181:397–405.
11. Gattone VH, II, Evan AP, Willis LR, Luft FC. Renal afferent arteriole in the spontaneously hypertensive rat. *Hypertension*. 1983;5:8–16.
12. Ahmed AK, Haylor JL, El Nahas AM, Johnson TS. Localization of matrix metalloproteinases and their inhibitors in experimental progressive kidney scarring. *Kidney Int*. 2007;71:755–763.
13. Ibrahim J, Berk BC, Hughes AD. Comparison of simultaneous measurements of blood pressure by tail-cuff and carotid arterial methods in conscious spontaneously hypertensive and Wistar-Kyoto rats. *Clin Exp Hypertens*. 2006;28:57–72.
14. Feihl F, Liaudet L, Levy BI, Waeber B. Hypertension and microvascular remodelling. *Cardiovasc Res*. 2008;78:274–285.
15. Sasamura H, Shimizu-Hirota R, Saruta T. Extracellular matrix remodeling in hypertension. *Curr Hypertens Rev*. 2005;1:51–60.
16. Woessner JF Jr. Matrix metalloproteinases and their inhibitors in connective tissue remodeling. *FASEB J*. 1991;5:2145–2154.
17. Mao D, Lee JK, VanVickle SJ, Thompson RW. Expression of collagenase-3 (MMP-13) in human abdominal aortic aneurysms and vascular smooth muscle cells in culture. *Biochem Biophys Res Commun*. 1999; 261:904–910.
18. Kelly BA, Bond BC, Poston L. Gestational profile of matrix metalloproteinases in rat uterine artery. *Mol Hum Reprod*. 2003;9:351–358.
19. Zijlstra A, Aimes RT, Zhu D, Regazzoni K, Kupriyanova T, Seandel M, Deryugina EI, Quigley JP. Collagenolysis-dependent angiogenesis mediated by matrix metalloproteinase-13 (collagenase-3). *J Biol Chem*. 2004;279:27633–27645.
20. Yu YM, Lin HC, Chang WC. Carnosic acid prevents the migration of human aortic smooth muscle cells by inhibiting the activation and expression of matrix metalloproteinase-9. *Br J Nutr*. 2008:1–8.
21. Guo RW, Yang LX, Li MQ, Liu B, Wang XM. Angiotensin II induces NF-kappa B activation in HUVEC via the p38MAPK pathway. *Peptides*. 2006;27:3269–3275.
22. Sasamura H, Nakaya H, Julius S, Takebayashi T, Sato Y, Uno H, Takeuchi M, Ishiguro K, Murakami M, Ryuzaki M, Itoh H. Short treatment with the angiotensin receptor blocker candesartan surveyed by telemedicine (STAR CAST) study: rationale and study design. *Hypertens Res*. 2008;31:1851–1857.

ONLINE SUPPLEMENT

'PULSE' TREATMENT WITH HIGH-DOSE ANGIOTENSIN BLOCKER REVERSES RENAL ARTERIOLAR HYPERTROPHY AND REGRESSES HYPERTENSION

Kimiko Ishiguro*, Kaori Hayashi*, Hiroyuki Sasamura, Yusuke Sakamaki, Hiroshi Itoh

Department of Internal Medicine, School of Medicine, Keio University, Tokyo, Japan

Correspondence to:

Hiroyuki Sasamura MD PhD

Department of Internal Medicine, School of Medicine, Keio University

35 Shinanomachi, Shinjuku-ku, Tokyo 160-8582, Japan

Tel: 81-3-5363-3796

Fax:81-3-3359-2745

E-mail: sasamura@sc.itc.keio.ac.jp

Running Title: Pulse ARB treatment in SHR

* These authors contributed equally to this study

Word counts: Manuscript 4334 words, Abstract 229 words

Group Number Treatment	1 WKY	2 SHR	3 SHR+ARB	4 SHR+CCB
Renal arterioles (30-100 um)	29.6±3.8	67.8±4.4*	36.5±4.2†	62.3±2.8*
Renal arterioles (100-300 um)	29.3±1.7	39.0±2.3	37.6±5.7	41.2±5.6
Mesenteric arterioles (30-100 um)	19.0±3.3	21.2±2.1	16.2±2.0	17.2±1.1
Mesenteric arterioles (100-300 um)	22.3±3.4	22.0±3.0	20.6±5.8	18.1±2.3
Cardiac arterioles (30-100 um)	17.5±3.4	24.9±2.1	20.1±1.9	25.1±2.0
Cardiac arterioles (100-300 um)	16.9±1.1	22.4±3.0	21.3.±1.6	25.4±1.0
Cerebral arterioles (30-100 um)	16.5±2.1	21.1±3.1	18.0±3.0	18.7±1.4
Cerebral arterioles (100-300 um)	16.1±1.9	19.9±3.0	21.4.±3.0	20.4±1.0

*: $p<0.01$ vs WKY ; † $p<0.01$ vs SHR

Online Supplement Table S1. Values of media/lumen ratios (x 100) of arterioles in the kidney, mesentery, heart, and brain in the different groups at age 18 weeks in Experiment 2. Results shown are means ± SEM. WKY: untreated WKY, SHR: untreated SHR, SHR+ARB: SHR treated with 'pulse' candesartan, SHR+CCB: SHR treated with 'pulse' nifedipine.

Neuroradiology (2008) 50:753–758
DOI 10.1007/s00234-008-0406-6

DIAGNOSTIC NEURORADIOLOGY

Discriminating between silent cerebral infarction and deep white matter hyperintensity using combinations of three types of magnetic resonance images: a multicenter observer performance study

Makoto Sasaki · Toshinori Hirai · Toshiaki Taoka · Shuichi Higano · Chieko Wakabayashi · Eiji Matsusue · Masahiro Ida

Received: 3 March 2008 / Accepted: 23 April 2008 / Published online: 12 June 2008

Abstract
Introduction We attempted to determine the most appropriate combination of magnetic resonance (MR) images that can accurately detect and discriminate between asymptomatic infarction and deep white matter hyperintensity (DWMH); these lesions have different clinical implications and are occasionally confused.

Materials and methods We performed an observer performance analysis using cerebral MR images of 45 individuals with or without asymptomatic small white matter infarction and/or mild DWMH who participated in a physical checkup program at four institutions. Six observers interpreted whether infarction and/or DWMH existed in combinations of two or three image types of the T1-weighted images (T1WI), T2-weighted images (T2WI), and fluid-attenuated inversion recovery (FLAIR) images. The observers' performance was evaluated with a receiver operating characteristic (ROC) analysis.
Results The averaged area under the ROC curve (Az) for detecting a infarction was significantly larger in the combination of all the three image types (0.95) than that in any combinations of the two image types (T1WI and FLAIR images, 0.87; T2WI and FLAIR images, 0.85; T1WI and T2WI, 0.86). The Az for detecting DWMH was significantly smaller in the combination of T1WI and T2WI (0.79) than that in other image combinations (T1WI and FLAIR, 0.89; T2WI and FLAIR, 0.91; T1WI, T2WI, and FLAIR, 0.90).
Conclusion The combination of T1WI, T2WI, and FLAIR images is required to accurately detect both small white matter infarction and mild DWMH.

Keywords Asymptomatic cerebral infarction · Deep white matter hyperintensity · Magnetic resonance imaging · Receiver operating characteristic analysis

M. Sasaki (✉)
Advanced Medical Research Center, Iwate Medical University, 19-1 Uchimaru, Morioka 020-8505, Japan
e-mail: masasaki@iwate-med.ac.jp

T. Hirai
Department of Diagnostic Radiology, Graduate School of Medical Sciences, Kumamoto University, 1-1-1 Honjo, Kumamoto 860-8556, Japan

T. Taoka
Department of Radiology, Nara Prefectural Medical University, 840 Shijo-cho, Kashihara 634-8521, Japan

S. Higano
Department of Diagnostic Radiology, Tohoku University School of Medicine, 1-1 Seiryo-cho, Sendai 980-8574, Japan

C. Wakabayashi
Department of Radiology, Suiseikai Kajikawa Hospital, 8-20 Showa-machi, Hiroshima 730-046, Japan

E. Matsusue
Division of Radiology, Department of Pathophysiological and Therapeutic Science, Faculty of Medicine, Tottori University, 36-1 Nishi-cho, Yonago 683-8504, Japan

M. Ida
Department of Radiology, Ebara Hospital, 4-5-10 Higashi-Yukigaya, Tokyo 145-0065, Japan

Introduction

Asymptomatic cerebral infarction and white matter hyperintensity are usually detected by magnetic resonance

imaging (MRI) in elderly individuals, particularly in those with hypertension. Silent lacunar infarction and marked white matter hyperintensity are known risk factors for the future occurrence of symptomatic/asymptomatic stroke and are associated with cognitive decline [1–3]. The MRI findings of lacunar infarction—a punctate/patchy configuration—are similar to those of mild deep white matter hyperintensity (DWMH) and dilated perivascular space (PVS) that are not considered to have substantial clinical significance [1, 4, 5]. Differentiating between small white matter infarction, mainly lacunar infarction, and mild DWMH is sometimes difficult because of the resemblance between them with regard to location, shape, and size; hence, interpretation of the signal characteristics of these lesions appears to be substantially crucial for the differentiation. One of the reasons for the confusion between these two types of lesions may be interinstitutional differences in the combination of the image types used for the interpretation of these lesions. The optimal combination of image types for the detection and differentiation of these lesions has not been determined. In this study, by using an observer performance analysis, we attempted to determine the most appropriate combination of T1-weighted images (T1WI), T2-weighted images (T2WI), and fluid-attenuated inversion recovery (FLAIR) images that would enable accurate evaluation and differentiation between small white matter infarction and DWMH.

Materials and methods

For the evaluation of observer performance concerning detection of the small infarction and mild DWMH, we recruited 45 healthy individuals without a history of stroke or any other neurological disorders who voluntarily underwent a physical checkup at four institutes at their own expense [27 men and 18 women; age, 49–80 years (mean, 64.4)]. The subjects included 40 individuals with unilateral or bilateral small white matter infarction, probably lacunar infarction, and/or DWMH of Fazekas grade 1 (punctuate foci) [6] as observed in MRI (24 men and 16 women; age, 49–80 years (mean, 65.2)] and five individuals without any lesions [three men and two women; age, 57–70 years (mean, 61.0)]. Axial spin-echo (SE) T1WI, fast SE (FSE) T2WI, and FLAIR images were obtained using 1.5-T superconductive MRI units [Signa MR/i (GE Healthcare, Milwaukee, WI, USA) was used at two institutes, Signa Excite (GE Healthcare) at one institute, and Magnetom Avanto (Siemens, Erlangen) at one institute]. The scanning parameters were as follows: 450–550/8–12 ms (repetition time/echo time) for T1WI; 2,800–4,200/88–104 ms (repetition time/effective echo time) for T2WI; 8,000–10,000/2,000–2,500/105–120 ms (repetition time/inversion time/effective echo time) for FLAIR; matrix size of 256×192–320×224; fields of view, 210–220 mm; and slice thickness, 5–6 mm with 1–1.5 mm interslice gaps; and 19–20 slices.

The images were collected as anonymized data of the Digital Imaging and Communication in Medicine (DICOM) format after receiving approval from the institutional review board by which the requirement for informed consent was waived. The image sections used for interpreting and confirming the presence or absence of infarction or DWMH were decided by a consensus of four senior neuroradiologists (T.H., T.T., S.H., M.I.) according to the draft criteria provided by the Committee for Development and Validation of Clinical Guidelines of the Japanese Society for Detection of Asymptomatic Brain Diseases that were developed for revising previous guidelines in an evidenced-based manner including a systematic critical reviewing of the previous reports (Table 1, Fig. 1), and they were blinded with regard to information concerning the subjects and institutes. We excluded five hemispheres because interpretation according to the criteria did not determine whether the lesion was an infarction or DWMH due to overlaps in signal characteristics, and 85 hemispheres (only infarction was present in ten hemispheres, only DWMH in 36, both infarction and DWMH in 14, and both lesions were not detected in 25) were evaluated for the analysis.

After consultation regarding the MRI findings of lacunar infarction or DWMH according to the criteria, six observers (two neuroradiologists, two neurologists, and two neurosurgeons) evaluated the confidence levels of the presence of the infarction and/or DWMH on the images. The experiments were performed four times with 1-month intervals. In each experiment, the following combination of images was used: (a) T1WI and FLAIR, (b) T2WI and FLAIR, (c) T1WI and T2WI, and (d) T1WI, T2WI, and FLAIR; the experiments were performed in different randomized orders and under anonymized conditions. The observers used the continuous confidence grading scale of a line-marking method to rate their confidence levels.

The likelihoods of infarction and DWMH were examined using a receiver operating characteristic (ROC) analysis performed with a LABROC software package, according to Metz et al. [7]. To evaluate the observers' performance with regard to the detection of infarction or DWMH, an area under the ROC curve (Az) of the six raters was compared between the four types of image combinations using repeated measures analysis of variance (ANOVA) with a post hoc least significant difference (LSD) test. Interrater agreements were evaluated with an intraclass correlation coefficient (ICC), and differences in ICC between the image combinations were examined using a repeated measures ANOVA with a post hoc LSD test. The alpha level used was 0.05.

Table 1 Differentiation between lacunar infarction, perivascular space, and white matter hyperintensity on MRI according to the draft clinical guidelines by the Japanese Society for Detection of Asymptomatic Brain Disease

	Lacunar infarction	Perivascular space	White matter hyperintensity
T1WI	Low	Iso—low	Iso—faintly low[a]
T2WI	High	High	Moderately high
PDWI	High w/wo low at the center	Iso—low	Moderately high
FLAIR	Iso—high w/wo low at the center	Iso—low	High
Size	≥3 mm	<3 mm[b]	Varied
Location	Cerebral white matter, basal ganglia (mainly in the upper two third), thalamus, pons	Cerebral white matter, basal ganglia (mainly in the lower one third), subinsular region, hippocampus, midbrain	Cerebral white matter, pontine-base

FLAIR fluid-attenuated inversion recovery, *PDWI* proton-density-weighted image, *T1WI* T1-weighted image, *T2WI* T2-weighted image, *w/wo* with or without

[a] The same as or higher than that for gray matter

[b] Can be greater than 10 mm in the lower one third of the basal ganglia

Results

The Az values of the six observers for detecting infarction in the combinations a, b, c, and d were 0.74–0.98 (mean, 0.87), 0.80–0.93 (mean, 0.85), 0.74–0.99 (mean, 0.86), and 0.89–1.00 (mean, 0.95), respectively; the averaged Az value in combination d was significantly larger than that obtained in the other image combinations ($P<0.05$, repeated measures ANOVA; Fig. 2). On the other hand, the Az values for the detection of DWMH in the combinations a, b, c, and d were 0.78–0.97 (mean, 0.89), 0.82–0.96 (mean, 0.91), 0.68–0.88 (mean, 0.79), and 0.72–0.97 (mean, 0.90), respectively;

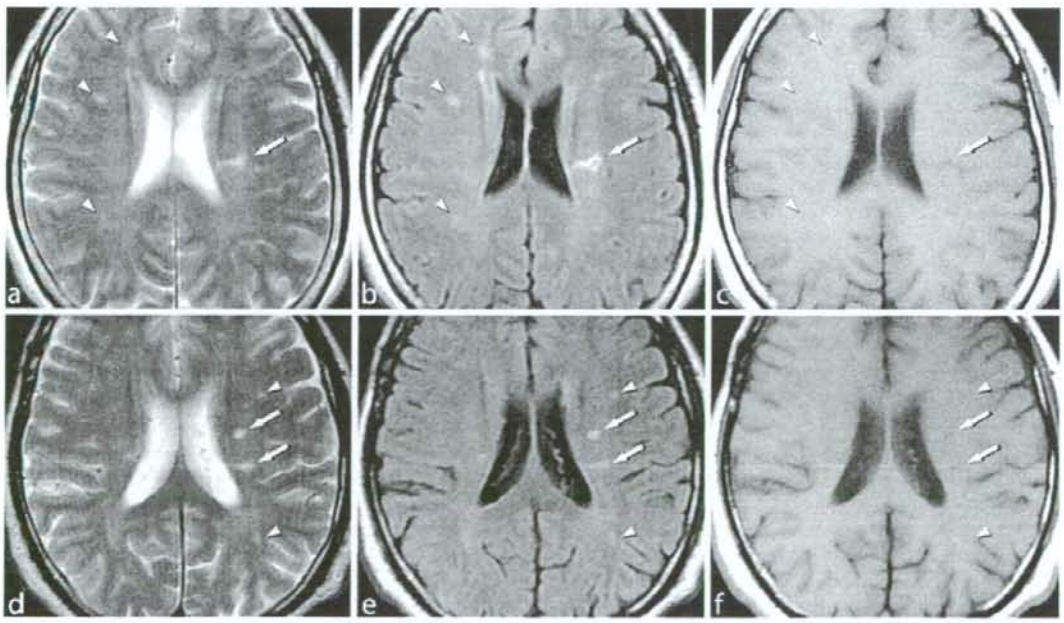

Fig. 1 Cerebral magnetic resonance images of the small white matter infarction and mild deep white matter hyperintensity (DWMH). **a**–**c** Fifty-nine-year-old man; **d**–**f** 63-year-old woman; **a**, **d** T2-weighted images (T2WI); **b**, **e** fluid-attenuated inversion recovery (FLAIR) images; and **c**, **f** T1-weighted images (T1WI). Infarctions show marked hyperintensity on T2WI, hyperintensity with or without central hypointensity on FLAIR images, and hypointensity on T1WI (*arrows*), whereas DWMHs show moderate hyperintensity on T2WI, hyperintensity on FLAIR images, and isointensity on T1WI (*arrowheads*)

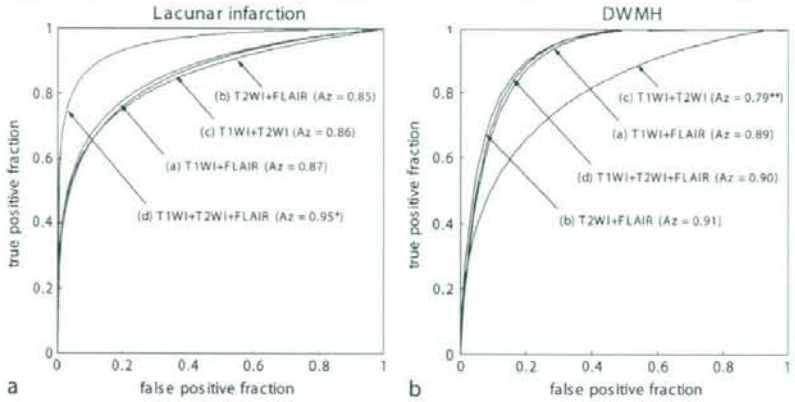

Fig. 2 Receiver operating characteristic (ROC) analysis of the visual assessment of the infarction and deep white matter hyperintensity (DWMH) in the elderly. **a** ROC curves for detecting infarction; **b** ROC curves for detecting DWMH. The Az value for detecting infarction in combination "d" of T1-weighted images (T1WI), T2-weighted images (T2WI), and fluid-attenuated inversion recovery (FLAIR) images is significantly larger than that obtained in the other image combinations, while that for the DWMH in combination "c" of T1WI and T2WI was significantly lower than those in other combinations. $^{*}P<0.05$, $^{**}P<0.01$

furthermore, the averaged Az value in combination c was significantly lower than those obtained in the other combinations ($P<0.01$, repeated measures ANOVA; Fig. 2).

With regard to interrater agreement, the ICCs for the infarcts for combinations a, b, c, and d between two of the six raters were 0.49±0.21, 0.58±0.12, 0.58±0.12, and 0.54±0.19 in the combinations of a, b, c, and d, respectively; there was no statistically significant difference between these values. The ICC values for DWMH were 0.52±0.16, 0.52±0.19, 0.24±0.16, and 0.58±0.22 for the combinations a, b, c, and d, respectively; and the ICC of combination c was significantly lower than those of other combinations ($P<0.01$, repeated measures ANOVA).

Discussion

Detection of asymptomatic infarction and marked white matter hyperintensity is one of the aims of performing cerebral MRI in elderly individuals because these lesions are considered to be risk factors for future stroke events. However, differentiation between lacunar infarction in the white matter and mild DWMH, which are substantially similar in their location, shape, and size, is sometimes difficult and may lead to misinterpretation and even unnecessary preventive medication. In this study, we successfully carried out observer-performance examinations for detecting and discriminating between small white matter infarction indicating lacunar infarction and mild DWMH by using MR images of subjects who underwent a physical checkup of the brain. We demonstrated that combination d, i.e., T1WI, T2WI, and FLAIR images, significantly improved the accuracy of identifying infarction as compared with other image combinations. We also demonstrated that image combinations that involved FLAIR images resulted in substantial improvement in the detection of DWMH and in the interrater agreement. These results suggested that signal characteristics in all the three types of images are crucial to accurate detection and discrimination between these two lesions. To the best of our knowledge, this is the first report that elucidates the importance of using an appropriate MRI suite for evaluating and differentiating between silent infarction and white matter hyperintensity.

Silent lacunar infarction is found in one fourth of healthy elderly individuals and has an incidence of approximately 20% every 5 years [8–10]; it increases the risk of stroke by two- to fourfold and is a well-known risk factor for future symptomatic stroke [1, 2]. On the other hand, DWMH is commonly observed in over 90% of the elderly population with an incidence of approximately 30% every 5 years [11, 12]. Severe DWMH has been reported to increase the risk of stroke by 3.5-fold as compared with mild DWMH that is considered to be merely an age-related change [2]. Hence, it is necessary to differentiate between silent lacunar infarction and mild DWMH when interpreting the cerebral MRI of the elderly; both lesions show similar findings but are different in clinical importance. Based on the results of this study, appropriate interpretation using three types of images can improve the accuracy of the differentiation and may help in predicting future symptomatic infarction.

To assist the differentiation between infarction and DWMH, we used the draft criteria developed by the Japanese Society for Detection of Asymptomatic Brain Diseases. As described in the criteria and previous studies

[5, 13–17], lacunar infarction usually shows marked hyperintensity on T2WI, varied signal—from isointensity to hyperintensity with or without central hypointensity—on FLAIR images, and hypointensity on T1WI due to T1 and T2 prolongations. DWMH shows moderate hyperintensity on T2WI, marked hyperintensity on FLAIR images, and isointensity or faint hypointensity on T1WI due to preferential moderate T2 prolongation. These findings that are characteristic of DWMH can be explained by the principal pathological change, i.e., myelin pallor (rarefaction of the myelin sheath without substantially increased intercellular space), although dilated PVS, vascular ectasia, arteriosclerosis, and occasionally, microscopic infarction and gliosis can coexist with the myelin pallor in DWMH [13–15]. The abovementioned differences in the signal characteristics of the three types of images between infarction and DWMH would be helpful for differentiating between these lesions in the elderly, which has been successfully validated in this study. However, relatively low interrater agreement in this study suggests that the differentiation using the criteria is unreliable in some cases, presumably because MR findings of these lesions can sometimes overlap. Further investigation is needed to overcome this issue.

One of limitations of this study is that, because it was retrospective, the imaging protocols were not standardized. The signal intensity of infarction and DWMH depends on scanning parameters, such as repetition time, echo time, and inversion time, particularly for the FLAIR images. Parameters such as in-plane spatial resolution, section thickness, and scanning plane can also affect the detectability of the lesions. A prospective study using standardized imaging protocols is required to diminish the biases related to the scanning parameters. Another limitation is that we did not evaluate proton-density-weighted images (PDWI), which had been adopted in previous cohort studies concerning lacunar infarction and white matter hyperintensity in the elderly [1, 2]. FLAIR images are usually used as an alternative to PDWI because lesions usually appear hyperintense, while the cerebrospinal fluid (CSF) appears hypointense in both images. However, it has been reported that these two types of images are different with regard to contrast and lesion conspicuity [18]. It remains unclear whether the diagnostic performance of the combination of T1WI, T2WI, and PDWI is better than that of T1WI, T2WI, and FLAIR images. Other limitations include the existence of patient selection bias due to the retrospective recruitment of volunteers from those who underwent physical checkup.

In conclusion, we determined that three types of images—T1WI, T2WI, and FLAIR—are required for accurately detecting both small white matter infarction and mild DWMH; these lesions have different clinical implications and are occasionally confused.

Acknowledgment Authors were grateful to Prof. Shigehiko Katsuragawa, Department of Radiological Technology, School of Health Sciences, Kumamoto University, for his generous help with the statistical analyses. This work was partly supported by a Grant for Leading Projects from the Japanese Society for Magnetic Resonance in Medicine and by a Grant-in-Aid for Science Research (18390256) and a Grant-in-Aid for Advanced Medical Science Research from the Ministry of Education, Culture, Sports, Science and Technology of Japan.

Conflict of interest statement We declare that we have no conflict of interest.

References

1. Bernick C, Kuller L, Dulberg C, Longstreth WT, Manolio T, Beauchamp N, Price T (2001) Silent MRI infarcts and the risk of future stroke: the Cardiovascular Health Study. Neurology 57:1222–1229
2. Vermeer SE, Hollander M, van Dijk EJ, Hofman A, Koudstaal PJ, Breteler MM (2003) Silent brain infarcts and white matter lesions increase stroke risk in the general population: the Rotterdam Scan Study. Stroke 34:1126–1129
3. van der Flier WM, van Straaten CW, Barkhof F, Verdelho A, Madureira S, Pantoni L, Inzitari D, Erkinjuntti T, Crisby M, Waldemar G, Schmidt R, Fazekas F, Scheltens P (2005) Small vessel disease and general cognitive function in nondisabled elderly: the LADIS study. Stroke 36:2116–2120
4. Pantoni L, Poggesi A, Basile AM, Pracucci G, Barkhof F, Chabriat H, Erkinjuntti T, Ferro JM, Hennerici M, O'Brien J, Schmidt R, Visser MC, Wahlund LO, Waldemar G, Wallin A, Inzitari D (2006) Leukoaraiosis predicts hidden global functioning impairment in nondisabled older people: the LADIS (leukoaraiosis and disability in the elderly) Study. J Am Geriatr Soc 54:1095–1101
5. Braffman BH, Zimmerman RA, Trojanowski JQ, Gonatas NK, Hickey WF, Schlaepfer WW (1988) Brain MR: pathologic correlation with gross and histopathology. 1. Lacunar infarction and Virchow–Robin spaces. AJR 151:551–558
6. Fazekas F, Chawluk JK, Alavi A, Hurtig HI, Zimmerman RA (1987) MR signal abnormalities at 1.5T in Alzheimer's dementia and normal aging. AJR 149:351–356
7. Metz CE, Herman BA, Shen JH (1998) Maximum-likelihood estimation of receiver operating characteristic (ROC) curves from continuously-distributed data. Stat Med 17:1033–1053
8. Longstreth WT, Bernick C, Manolio TA, Bryan N, jungreis CA, Price TR (1998) Lacunar infarcts defined by magnetic resonance imaging of 3660 elderly people: the Cardiovascular Health Study. Arch Neurol 55:1217–1225
9. Longstreth WT, Dulberg C, Manolio TA, Lewis MR, Beauchamp NJ, O'Leary D, Carr J, Furberg CD (2002) Incidence, manifestations, and predictors of brain infarcts defined by serial cranial magnetic resonance imaging in the elderly: the Cardiovascular Health Study. Stroke 33:2376–2382
10. Vermeer SE, den Heijer T, Koudstaal PJ, Oudkerk M, Hofman A, Breteler MMB (2003) Incidence and risk factors of silent brain infarcts in the population-based Rotterdam Scan Study. Stroke 34:392–396
11. de Leeuw FE, de Groot JC, Achten E, Oudkerk M, Ramos LM, Heijboer R, Hofman A, Jolles J, van Gijn J, Breteler MM (2001) Prevalence of cerebral white matter lesions in elderly people: a population based magnetic resonance imaging study. The Rotterdam Scan Study. J Neurol Neurosurg Psychiatr 70:9–14

12. Longstreth WT, Arnold AM, Beauchamp NJ Jr, Manolio TA, Lefkowitz D, Jungreis C, Hirsch CH, O'Leary DH, Furberg CD (2005) Incidence, manifestations, and predictors of worsening white matter on serial cranial magnetic resonance imaging in the elderly: the Cardiovascular Health Study. Stroke 36:56–61
13. Awad IA, Johnson PC, Spetzler RF, Hodak JA (1986) Incidental subcortical lesions identified on magnetic resonance imaging in the elderly. II. Postmortem pathological correlations. Stroke 17:1090–1097
14. Chimowitz MI, Estes ML, Furlan AJ, Awad IA (1992) Further observations on the pathology of subcortical lesions identified on magnetic resonance imaging. Arch Neurol 49:747–752
15. Matsusue E, Sugihara S, Fujii S, Ohama E, Kinishita T, Ogawa T (2006) White matter changes in elderly people: MR-pathologic correlations. Magn Reson Med Sci 5:99–104
16. Shinohara Y, Tohgi H, Hirai S, Terashi A, Fukuuchi Y, Yamaguchi T, Okudera T (2007) Effect of the Ca antagonist nilvadipine on stroke occurrence or recurrence and extension of asymptomatic cerebral infarction in hypertensive patients with or without history of stroke (PICA study). Cerebrovasc Dis 24: 202–209
17. Bokura H, Kobayashi S, Yamaguchi S (1998) Distinguishing silent lacunar infarction from enlarged Virchow-Robin spaces: a magnetic resonance imaging and pathological study. J Neurol 245:116–122
18. Okuda T, Korogi Y, Shigematsu Y, Sugahara T, Hirai T, Ikushima I, Lian L, Takahashi M (1999) Brain lesions: when should fluid-attenuated inversion recovery sequences be used in MR evaluation? Radiology 212:793–798

Radiat Med (2008) 26:33–38
DOI 10.1007/s11604-007-0184-9

CASE REPORT

Multiple cerebral aneurysms associated with Takayasu arteritis successfully treated with coil embolization

**Katsutoshi Takayama · Hiroyuki Nakagawa
Satoru Iwasaki · Toshiaki Taoka · Kaoru Myouchin
Takeshi Wada · Masahiko Sakamoto · Akio Fukusumi
Shinichiro Kurokawa · Kimihiko Kichikawa**

Received: May 25, 2007 / Accepted: August 7, 2007

Abstract The cerebrovascular complications of Takayasu arteritis are primarily related to the presence of occlusive lesions. Cerebral aneurysms rarely occur as complications; only 18 cases have been reported thus far. The use of coil embolization to treat cerebral aneurysms occurring as a complication of Takayasu arteritis has not been previously reported. We report a case of Takayasu arteritis with a basilar tip aneurysm and a P1 segment aneurysm of the left posterior cerebral artery that were successfully treated with coil embolization. Because coil embolization for cerebral aneurysms associated with Takayasu arteritis requires the use of limited access routes that have extremely curved and tortuous courses, catheter navigation was difficult. The guide catheter, microcatheter, and guidewire must be selected and navigated with greater care than is usually required for common aneurysm embolization.

Key words Takayasu arteritis · Takayasu's disease · Aortitis syndrome · Cerebral aneurysm · Endovascular treatment

K. Takayama (✉)
Department of Interventional Neuroradiology, Ishinkai Yao General Hospital, 1-41 Numa, Yao 581-0036, Japan
Tel. +81-729-48-2500; Fax +81-729-48-7950
e-mail: takayamaneuroivs@par.odn.ne.jp

H. Nakagawa · S. Iwasaki · T. Taoka · K. Myouchin · T. Wada · M. Sakamoto · A. Fukusumi · K. Kichikawa
Department of Radiology, Nara Medical University, Kashihara, Japan

S. Kurokawa
Department of Neurosurgery, Ishinkai Yao General Hospital, Yao, Japan

Introduction

Takayasu arteritis is a systemic vasculitis of unknown etiology that mainly affects the aorta, its major branches, and the pulmonary artery. Stenosis or occlusion of the major branches of the aorta causes various clinical manifestations, mostly involving symptoms of cerebrovascular insufficiency.[1] Intracranial cerebral aneurysms are rarely associated with Takayasu arteritis, with only 18 cases having been previously reported.[1–16] Endovascular treatment for intracranial cerebral aneurysms associated with Takayasu arteritis has never been previously reported. We report the successful endovascular treatment of a patient with multiple intracranial cerebral aneurysms associated with Takayasu arteritis.

Case report

A 70-year-old woman presented with headache. Ten years earlier, she was diagnosed as having Takayasu arteritis, hypertension, atrial fibrillation, and aortic valve insufficiency. Screening magnetic resonance (MR) angiography for headache revealed an occlusion of the right internal carotid artery and aneurysms located on the tip of the basilar artery and the left posterior cerebral artery (Fig. 1). The patient was admitted for further evaluation. On admission, the neurological examination was normal. Laboratory data did not reveal any definitive abnormality, including C-reactive protein, indicating that there was no active inflammation.

Cerebral angiography on admission showed the following: The aortogram demonstrated occlusion of the origin of the right common carotid artery, severe stenosis of the left common carotid artery, and occlusion

Fig. 1. Cranial magnetic resonance angiography (MRA), frontal view, shows that the right internal carotid artery is not visualized. Note a saccular, small, narrow-necked aneurysm on the P1 segment of the left posterior cerebral artery (*arrowhead*) and a wide-necked aneurysm on the basilar tip (*arrow*)

immediately before the carotid bifurcation (Fig. 2A). On left subclavian angiography, occlusion of the distal portion of the left vertebral artery was observed, and the occipital artery was visualized through the collateral circulation from the vertebral artery and the deep cervical artery. The external carotid artery is visualized by retrograde flow from the occipital artery. The left internal carotid artery was opacified anterogradely from the external carotid artery (Fig. 2D). On right vertebral angiography, part of the left middle cerebral artery, the right middle cerebral artery, and the bilateral anterior cerebral arteries were visualized via the basilar and posterior communicating arteries; saccular aneurysms with diameters of 3 and 4 mm, respectively, were observed in the P1 segment of the left posterior cerebral artery and the basilar tip, respectively (Fig. 2B, C). The right vertebral artery supplies blood flow to almost the entire brain. The overall schema is shown in Fig. 3.

We explained to the merit and the demerit of each endovascular and surgical approach considering the aneurysmal location, shape, and tortuosity of the access route to the patient with a neurosurgeon, and the patient chose to have endovascular treatment.

Three days prior to the procedure, aspirin (100 mg/day) and cilostazole (200 mg/day) were prescribed. Under general anesthesia, both aneurysms were treated with coil embolization. Heparin was given intravenously as 3000- and 1000-IU boluses every hour to achieve a periprocedural activated clotting time of >250 s. A 4F catheter (Cathex; Cathex, Sagamihara, Japan) was advanced into a 6F catheter (Envoy, Cordis; Neurovascular, Miami Lakes, FL, USA) coaxially with a 0.035-inch Lubflow guide wire (Toray Medical, Tokyo, Japan) in the right vertebral artery via the right femoral approach. However, a 6F catheter could not be selectively introduced into the right vertebral artery because the right subclavian artery and the origin of the right vertebral artery were extremely tortuous (Fig. 4A). Thus, a 0.035-inch Amplatz guidewire (Cook, Bloomington, IN, USA) was used. A 6F catheter could not be introduced to the distal portion of the right vertebral artery (Fig. 4A). First, an Excelsior SL-10 microcatheter (Boston Scientific, Fremont, CA, USA) was introduced through a 6F right vertebral artery catheter; then, using a 0.014-inch guidewire (Transcend; Boston Scientific), a microcatheter was inserted into the distal aneurysm located in the left posterior cerebral artery. However, due to the highly curved vertebral artery and the effects of duplication of the right vertebral artery, catheter navigation was extremely difficult (Fig. 4B). Three Guglielmi detachable coils (GDCs) (Boston Scientific: GDC-10 soft 2D SR 3 mm × 6 cm; GDC-10 ultra-soft 2 mm × 3 cm; GDC-10 ultra-soft 2 mm × 2 cm) were deployed and detached. The aneurysm was occluded with a mild neck remnant (Fig. 4C). Although the same microcatheter and microguidewire were maneuvered near the aneurysm located at the basilar tip, a microcatheter could not be placed in the aneurysm. Because the microcatheter memorized the shape of the tortuous vessel, trackability was decreasing. Thus, a 6F catheter was moved to the right subclavian artery. We changed to a new 6F catheter (Guider; Boston Scientific) and a new microcatheter (Excelsior 10/18; Boston Scientific). A microcatheter was placed in the aneurysm. Three GDCs (GDC-10 3D SR 4 mm × 6 cm; GDC-10 ultra-soft 3 mm × 8 cm; GDC-10 ultra-soft 2 mm × 4 cm) were deployed and detached. A minor body filing of the aneurysm was obtained (Fig. 4C). The patient's postoperative course was uneventful, and she was discharged with no neurological deficit 1 week later.

Discussion

Cerebrovascular lesions associated with Takayasu arteritis include stenosis and occlusive lesions. Cerebral aneurysms are rarely associated with Takayasu arteritis, with only 19 cases (31 aneurysms) including the present case.[1,16] (Table 1). In total, 16 aneurysms (51.6%) occurred in the vertebrobasilar arterial system and 15 (48.4%) in the anterior circulation. Altogether, 9 of 19

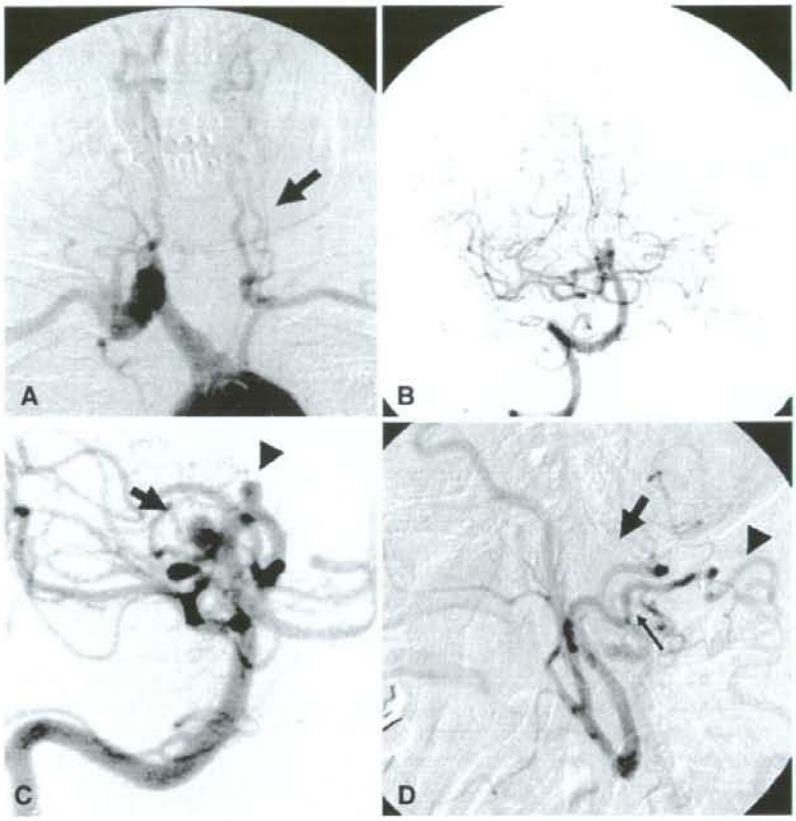

Fig. 2. Cerebral angiography. **A** Aortogram, frontal view. The right common carotid artery is occluded at the origin. The left common carotid artery is extremely narrow and is occluded immediately prior to the carotid bifurcation (*arrow*). **B** Right vertebral angiogram, frontal view. The bilateral anterior cerebral arteries, right middle cerebral artery, and part of the left middle cerebral artery are visualized via the bilateral posterior communicating arteries. **C** Right vertebral angiogram in the right anterior oblique view demonstrates a saccular narrow-necked aneurysm with a diameter of 3 mm at the P1 segment of the left posterior cerebral artery (*arrowhead*) and a wide-necked aneurysm with a 4-mm diameter at the basilar tip (*arrow*). **D** Left subclavian angiogram, lateral view. The distal portion of the left vertebral artery is occluded (*thick arrow*). The external carotid artery is visualized by retrograde flow from the occipital artery (*thin arrow*) through collateral circulation from the vertebral artery and the deep cervical artery (*arrowhead*). The left internal carotid artery is opacified and shows anterograde flow via the left external carotid artery

patients (47.4%) had multiple aneurysms. Cerebral aneurysms naturally arise in the vertebrobasilar arterial system and the anterior circulation at rates of 9.6% and 90.4%, respectively; and 24.2% of patients develop multiple aneurysms.[17,18] Thus, patients with cerebral aneurysms associated with Takayasu arteritis have a high rate of multiplicity, and these aneurysms commonly occur in the vertebrobasilar arterial system.

The incidence of cerebral aneurysm associated with Takayasu arteritis is unclear; however, autopsy findings indicate that 1 of 26 (3.8%) patients[19] and 0 of 77 patients[20] with Takayasu arteritis had cerebral aneurysms. According to statistics provided by Japan's Ministry of Health, Labor, and Welfare in 1992, it was estimated that, in Japan, approximately 5000 patients have Takayasu arteritis, and 100–200 new cases occur each year; there is a 9.4-fold greater incidence among women compared to men.[21] Based on our review of the literature, there were 19 cases of cerebral aneurysms reported in the last 35 years; the incidence of aneurysm among Takayasu arteritis patients ranged between 0.27% and 0.54%. This range appears to be comparable to the spontaneous incidence of cerebral aneurysm (0.6%–1.5%) generally reported.[22] However, given that many aneurysms

associated with Takayasu arteritis present with subarachnoid hemorrhage,[1,7,9,15] the incidence of unruptured aneurysms, such as those found in the present case, is thought to be higher.

At autopsy, the absence of inflammatory changes in the cerebral aneurysms and the surrounding vessels suggests that cerebral aneurysms associated with Takayasu arteritis are not likely to result from vasculitis.[13] In Takayasu arteritis, the increased incidence of vertebrobasilar aneurysms is attributed to the presence of hemodynamic stress, which is produced by stenosis and occlusion of arteries, such as the common carotid and subclavian arteries, which act on the vertebral artery; and the vertebral artery is thought to be the least likely to be affected by Takayasu arteritis.[1] Our patient had bilateral carotid artery occlusion; hemodynamic stress caused by intracranial blood flow that was maintained via the right vertebral artery was thought to have led to the formation of aneurysms at the tip of the basilar artery and the left posterior cerebral artery.

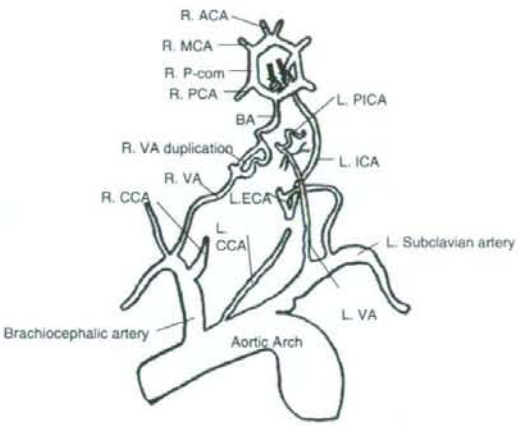

Fig. 3. Schema of cervical arteries and cerebral arteries. The left and right common carotid arteries are occluded. Aneurysms are seen in the basilar tip and the P1 segment of the left posterior cerebral artery (*arrows*). *P-com*, posterior communicating artery; *ICA*, internal carotid artery; *MCA*, middle cerebral artery; *ACA*, anterior cerebral artery; *BA*, basilar artery; *VA*, vertebral artery; *PICA*, posterior inferior cerebellar artery; *PCA*, posterior cerebral artery; *R.*, right; *L.*, left; *CCA*, common carotid artery

Posterior circulation aneurysms, as in this case, particularly those located at the tip of the basilar artery, are associated with less favorable outcomes following surgical clipping than those located at other sites because those aneurysms are located deep in the brain, and perforating vessels are located in the vicinity.

Batjer et al.[23] assessed 126 patients with ruptured aneurysms of the distal basilar artery and reported 11% morbidity and 8% mortality. In another study of 99 cases with unruptured basilar tip aneurysms (small, $n = 71$; large, $n = 28$) treated by surgical clipping performed by highly skilled neurosurgeons, 15.2% of cases had postoperative onset of neurological symptoms, with 6.1% morbidity and 0%mortality[24] Tateshima et al.[25] used coil embolization to treat basilar tip aneurysms; they reported successful embolization in 94.7% of 75 aneurysms (complete or nearly complete occlusion in 85.3% of aneurysms), with 4.1% morbidity and 1.4% mortality. Henkes et al.[26] reported successful embolization in 98% of 316

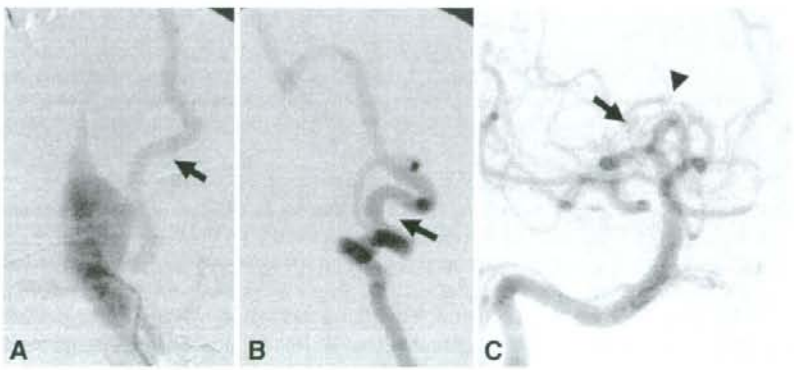

Fig. 4. **A** Right subclavian angiogram, left anterior oblique view. The guide catheter could be inserted only at the C7 level (*arrow*) owing to the steep curvature of the right subclavian artery and the origin of the vertebral artery. **B** Right vertebral angiogram, lateral view. Duplication of the right vertebral artery is shown. The thicker artery enters the spinal canal at the C1–2 level, creating a steep curve; the catheter is introduced here (*arrow*). **C** Right vertebral angiogram immediately after coil embolization in a right anterior oblique view demonstrates minor body filling of the basilar tip aneurysm (*arrow*) and a minor neck remnant of the P1 segment aneurysm of the left posterior cerebral artery (*arrowhead*)

Table 1. Summary of reported cases of Takayasu arteritis associated with cerebral aneurysm

Report	Year	Age/sex	Symptom	Location of aneurysm	Treatment for aneurysm	Outcome	Angiographic findings			
							CCA		VA	
							Rt.	Lt	Rt.	Lt
1. Niitsu[15]	1972	26/F	SAH	Lt. ICA-PComA	None	Death	Oc.	St.	St.	Oc
2. Izawa[3]	1980	55/F	SAH	VA union	None	No recurrence	Pa.	Oc.	Oc.	Pa.
3. Kumagai[14]	1981	41/F	SAH	BA tip, Rt. PCA-PComA	Clipping	Cure	Pa.	Oc.	Pa.	Oc.
4. Kumagai[14]	1981	55/F	SAH	BA-Rt. SCA, Lt. SCA	None	Death	Oc.	Oc.	Pa.	Oc.
5. Arita[16]	1981	48/F	Incidental	AComA, AComA	Clipping	Cure	Pa.	Pa.	Oc.	St.
6. Imaizumi[2]	1982	48/F	SAH	AComA	Clipping	Cure	Oc.	Pa.	St.	Pa.
7. Matsuzawa[7]	1982	26/F	SAH	Lt. IC-PComA, Lt. ICA	None	Death	St.	Pa.	St.	Oc.
8. Matsuzawa[7]	1982	54/F	SAH	BA tip	None	Death	Oc.	Oc.	Pa.	Pa.
9. Satoh[6]	1983	38/F	SAH	ACA (A1)	Clipping	Cure	Pa.	St.	Pa.	St.
10. Matsuzawa[10]	1984	55/M	SAH	Rt. VA-PICA	None	Death	Pa.	Oc.	Pa.	St.
11. Wakabayashi[4]	1985	56/F	SAH	BA tip	None	Death	Oc.	Oc.	Pa.	Pa.
12. Mizuno[12]	1985	55/F	SAH	BA-Rt.PCA	None	No recurrence	Pa.	Oc.	Pa.	St.
13. Matsuzawa[11]	1986	64/F	SAH	Lt. IC-Oph A, Lt. ICA-PComA, BA tip, BA-Lt. AICA	Clipping	Cure	Oc.	Pa.	Pa.	St.
14. Kurimoto[5]	1987	48/F	SAH	AComA	Clipping	Cure	Pa.	Pa.	Pa.	St.
15. Sunami[1]	1987	55/F	SAH	VA union, Rt. PCA	None	no recurrence	Oc.	Pa.	Oc.	Pa.
16. Nishimura[9]	1994	48/F	SAH	AComA, Rt. MCA, Lt. IC top	Clipping	Cure	Pa.	Pa.	Pa.	Pa.
17. Asaoka[8]	1998	54/F	Incidental	AComA, Lt. ICA	Clipping	Cure	St.	Pa.	Pa.	Oc.
18. Kanda[13]	2004	48/F	SAH	Rt. VA-PICA	Clipping	Cure	St.	St.	Pa.	Oc.
19. Present study	2007	70/F	Incidental	BA-tip, Lt. PCA(P1)	Coiling	Cure	Oc.	Oc.	Pa.	Pa.

AComA, anterior communicating artery; PComA, posterior communicating artery; ICA, internal carotid artery; MCA, middle cerebral artery; ACA, anterior cerebral artery; BA, basilar artery; VA, vertebral artery; PICA, posterior inferior cerebellar artery; AICA, anterior inferior cerebellar artery; PCA, posterior cerebral artery; SCA, superior cerebellar artery; Oph, ophthalmic artery; SAH, subarachnoid hemorrhage; Oc., occlusion; Pa. patent; St., stenosis; Rt., right; Lt., left; CCA, common carotid artery

aneurysms (complete or nearly complete occlusion in 86.0% of aneurysms), with 5.4% morbidity and 2.2% mortality. Given these favorable outcomes of the initial treatment of basilar tip artery aneurysms, coil embolization is seen as a new treatment method that may replace surgical clipping. Although long-term stability following coil embolization has not yet been determined, follow-up (mean 18.6 months) angiograms after coil embolization for basilar tip aneurysms showed complete or nearly complete occlusion in 71.4% of aneurysms. In particular, the complete occlusion rate was 92% in small aneurysms (≤1 cm), which indicates favorable long-term stability.[25]

In the present case, because of occlusion of the left vertebral artery, coil embolization had to be performed using the right vertebral artery as the access route; however, the right vertebral artery was extremely curved and tortuous at both the origin and the distal portion. Given that the guide catheter could only be placed proximal to the vertebral artery, as well as the much-curved course of the vertebral artery, at first we treated the distal aneurysm to avoid interference with microcatheter manipulation by the primary embolized aneurysm. We tried to approach the second aneurysm with the same microcatheter, but it was difficult to insert it into the aneurysm. Because the catheter and wire had memorized the shape of the tortuous vessel, they could not be used for insertion into the second aneurysm. We then introduced the microcatheter into the second aneurysm using new equipment.

Because coil embolization for cerebral aneurysms associated with Takayasu arteritis requires the use of limited access routes that have highly curved and tortuous courses, the guide catheter, microcatheter, and guidewire must be selected and navigated with greater care than is usually required for common aneurysm embolization.

References

1. Sunami N, Yamamoto Y, Kunishio K, Yamamoto Y, Okamoto Y, Asari S. A case of aortitis syndrome with a ruptured cerebral aneurysm. Rinsho Hoshasen 1987;32:119–22.
2. Imaizumi S, Nagamine Y, Nakamura N, Katakura R, Higuchi H. Aneurysm of anterior communicating artery associated with aortitis syndrome—a treated case by aneurysmal neck clipping [author's translation]. No Shinkei Geka 1982;10: 449–55.
3. Kurimoto M ES, Arai K, Oka N, Takaku A. Aortitis syndrome associated with a ruptured anterior communicating

artery aneurysm and hypertensive intracerebral hemorrhage: case report. Neurol Med Chir (Tokyo) 1987;27:139–43.
4. Wakabayashi T, Urui S. Basilar artery aneurysm associated with megadolichobasilar anomaly in pulseless disease. Rinsho Hoshasen 1985;30:1009–11.
5. Izawa M, Okino T, Kagawa M, Kitamura K. A case of aortitis syndrome associated with basilar aneurysm. No Shinkei Geka 1980;8:1071–6.
6. Satoh T, Yamamoto Y, Asari S, Tomida Y, Ogura T. A case of aortitis syndrome with a ruptured cerebral aneurysm. No Shinkei Geka 1983;11:305–10.
7. Matsuzawa T SH, Sato F, Furuse M, Fukushima K. The development of intracranial aneurysms associated with pulseless disease. Surg Neurol 1982;17:132–6.
8. Asaoka K, Houkin K, Fujimoto S, Ishikawa T, Abe H. Intracranial aneurysms associated with aortitis syndrome: case report and review of the literature. Neurosurgery 1998;42: 157–60.
9. Nishimura S, Suzuki M, Mizoi K, Yoshimoto T. Multiple cerebral aneurysms associated with aortitis syndrome—case report. Neurol Med Chir (Tokyo) 1994;34:821–4.
10. Masuzawa T, Shimabukuro H, Furuse M, Fukushima K, Kasuda H, Sato F. Pulseless disease associated with a ruptured intracranial vertebral aneurysm. Neurol Med Chir (Tokyo) 1984;24:490–4.
11. Masuzawa T, Kurokawa T, Oguro K, Saito K, Miura H, Furuse M, et al. Pulseless disease associated with multiple intracranial aneurysms. Neuroradiology 1986;28:17–22.
12. Mizuno M, Yamanouchi Y, Oka N, Someda K, Matsumura H. Ruptured cerebral aneurysm associated with aortitis syndrome: a case report. No Shinkei Geka 1985;13:661–7.
13. Kanda M, Shinoda S, Masuzawa T. Ruptured vertebral artery-posterior inferior cerebellar artery aneurysm associated with pulseless disease—case report. Neurol Med Chir (Tokyo) 2004;44:363–7.
14. Kumagai Y, Sugiyama H, Nawata H, et al. Two cases of pulseless disease with cerebral aneurysm [author's translation]. No Shinkei Geka 1981;9:611–5.
15. Niitsu K, Aimoto H, Nose T, et al. An autopsy case of aortic syndrome with cerebral aneurysm and aortic dissection. Medicina 1972; 9:1898–1902.
16. Arita M NT, Ryono M, Minakata T, Nishio I, Masuyama Y. A case of arotitis syndrome with asymmetrical septal hypertrophy and cerebral aneurysm. Shinzou 1981;13:490–494.
17. Yasagil M. Multiple aneurysms. In: Microneurosurgery. New York: Georg Thieme Verlag; 1984.
18. Yasargil M. Pathological considerations. in: Microneurosurgery. New York: Georg Thieme Verlag; 1984.
19. Saito K. Clinicopathological syudy of twnety-six autopsy cases of Takayasu's arteritis Cardioangiology 1979;6:149–58.
20. Sano K, Saito I. Pulseless disease: summary of our experiences and studies. Schweiz Arch Neurol Neurochir Psychiatr 1972;111:417–33.
21. Koide K. Takayasu arteritis in Japan. Heart Vessels Suppl 1992;7:48–54.
22. Winn HR, Jane JA Sr, Taylor J, Kaiser D, Britz GW. Prevalence of asymptomatic incidental aneurysms: review of 4568 arteriograms. J Neurosurg 2002;96:43–9.
23. Batjer HH, Samson DS. Causes of morbidity and mortality from surgery of aneurysms of the distal basilar artery. Neurosurgery 1989;25:904–15.
24. Rice BJ, Peerless SJ, Drake CG. Surgical treatment of unruptured aneurysms of the posterior circulation. J Neurosurg 1990;73:165–73.
25. Tateshima S, Murayama Y, Gobin YP, Duckwiler GR, Guglielmi G, Vinuela F. Endovascular treatment of basilar tip aneurysms using Guglielmi detachable coils: anatomic and clinical outcomes in 73 patients from a single institution. Neurosurgery 2000;47:1332–9.
26. Henkes H, Fischer S, Mariushi W, Weber W, Liebig T, Miloslavski E, et al. Angiographic and clinical results in 316 coil-treated basilar artery bifurcation aneurysms. J Neurosurg 2005;103:990–9.

Circ J 2009; **73:** 336–342

Clopidogrel Resistance in Japanese Patients Scheduled for Percutaneous Coronary Intervention

Kozo Hoshino, MD; Hisanori Horiuchi, MD; Tomohisa Tada, MD; Junichi Tazaki, MD; Eiichiro Nishi, MD; Mitsunori Kawato, MD; Tomoyuki Ikeda, MD; Hiromi Yamamoto, MD; Masaharu Akao, MD; Yutaka Furukawa, MD; Satoshi Shizuta, MD; Masanao Toma, MD; Toshihiro Tamura, MD; Naritatsu Saito, MD; Takahiro Doi, MD; Neiko Ozasa, MD; Toshikazu Jinnai, MD; Kanako Takahashi, MT; Haruyo Watanabe, MT; Yuka Yoshikawa, MT; Naoko Nishimoto, MT; Chiho Ouchi, MT; Takeshi Morimoto, MD*; Toru Kita, MD; Takeshi Kimura, MD

Background Dual antiplatelet therapy with acetylsalicylic acid (ASA) and a P2Y12 ADP-receptor blocker is standard for prevention of coronary stent thrombosis. Clopidogrel, a 2nd-generation P2Y12 blocker, has recently become available in Japan and this study aimed to evaluate its antiplatelet effects in Japanese patients.

Methods and Results Thirty Japanese patients scheduled for elective coronary stent implantation were enrolled. Under low-dose ASA therapy, 300 mg clopidogrel was loaded on the 1st day and a daily 75-mg dose was administered on the following days. Assessed by optical aggregometer, rapid inhibition occurred at 4 h, when the inhibition of platelet aggregation rate (IPA) was 16.4±12.8% using 5 μmol/L ADP as the stimulus. The antiplatelet efficacy of clopidogrel was reasonably constant in each patient throughout the study period, although there was a broad inter-individual variation. At 48 h after clopidogrel loading, the ratios of responders (IPA ≥30%), hypo-responders (10%≤IPA<30%), and non-responders (IPA <10%) were 36%, 50%, and 14%, respectively.

Conclusions The antiplatelet effectiveness of clopidogrel appeared individual-specific with wide inter-individual variation. The rate of clopidogrel non-responders was 14% among the examined Japanese patients. (*Circ J* 2009; **73:** 336–342)

Key Words: Adenosine diphosphate; Antiplatelet drug; Clopidogrel; Coronary stent; Thienopiridine

Percutaneous coronary intervention (PCI) with coronary stent implantation is performed worldwide for ischemic heart disease. In Japan, 153,501 patients underwent this therapy in 2006, as described in the surveillance report from the Japan Circulation Society. One of the most serious problems is acute and late thrombosis at the site of stenting and much effort had been made to avoid this critical complication. The current standard dual antiplatelet therapy with acetylsalicylic acid (ASA) and thienopyridine ADP-receptor blocker has proven to be a powerful preventive solution[1–5]

Two thienopyridine antiplatelet agents are currently available: ticlopidine and clopidogrel. Although ticlopidine, a 1st-generation thienopyridine, has contributed much to the prevention of stent thrombosis, it frequently causes adverse side-effects such as agranulocytosis, thrombotic thrombocytopenic purpura and liver injury. Clopidogrel, a 2nd-generation P2Y12 blocker, has a better safety profile with a lower incidence of hematologic and liver complications, and has now largely replaced ticlopidine in clinical practice.

One important problem with clopidogrel is the wide inter-individual variation in its antiplatelet effect[3,6–8] It has been demonstrated that clopidogrel does not exert an antiplatelet effect in a certain proportion of patients in Western populations[9] known as clopidogrel resistance. Importantly, several studies have revealed that cardiovascular risk is elevated in patients with clopidogrel resistance[10]

On the other hand, there are well-established differences in the atherothrombotic and hemorrhagic risks in the Japanese compared with Western populations[11] so results from clinical trials in the West using novel antithrombotic agents cannot be applied directly to Japanese patients. Furthermore, the standard dose of ticlopidine for the Japanese (200 mg/day) is much lower than that for Western people (500 mg/day), but the same daily maintenance dose (75 mg) of clopidogrel is used in both populations. Therefore, some Japanese physicians are concerned about the strength of the effect of clopidogrel in Japanese patients and because of those concerns, we designed the present study to evaluate the antiplatelet effects of clopidogrel under low-dose ASA therapy in 30 Japanese patients scheduled for PCI.

Methods

Study Protocol

This study was approved by the Ethics Committee of Kyoto University Hospital, and written informed consent was given by all enrolled patients, who were undergoing elective

(Received June 11, 2008; revised manuscript received August 21, 2008; accepted September 16, 2008; released online December 24, 2008)
*Department of Cardiovascular Medicine, *Center for Medical Education, Graduate School of Medicine, Kyoto University, Kyoto, Japan*
Mailing address: Hisanori Horiuchi, MD, Department of Cardiovascular Medicine, Graduate School of Medicine, Kyoto University, 54 Shogoin, Kawahara-cho, Kyoto 606-8507, Japan. E-mail: horiuchi@kuhp.kyoto-u.ac.jp

coronary stent implantation. The initial diagnosis of ischemic heart disease was based on symptoms, a non-invasive examination such as stress electrocardiogram, and/or coronary computed tomography angiography. Further entry criteria were (1) ASA (81–100 mg/daily) for at least 7 days prior to the initial cardiac catheterization and (2) platelet count of 100–350×10⁹/L and hemoglobin ≥10 g/dl. Exclusion criteria were: (1) recent bleeding diathesis; (2) hematologic or malignant disorder; (3) oral anticoagulation with coumarin derivatives; (4) glycoprotein IIb/IIIa inhibitor or fibrinolytics administered during either the PCI or the preceding 14 days; and (5) antiplatelet therapy with thienopyridines, cilostazol or dypridimole within the preceding 28 days.

A loading dose of 300 mg clopidogrel was administered on the 1st day, approximately 24 h before PCI. A daily maintenance dose (75 mg) was administered the morning before the procedure and continued thereafter. ASA was administered at a daily dose of 81–100 mg. Blood samples were collected at enrolment, and at 4 (3–5) h, 24 (22–26) h and 48 (46–50) h after the loading dose (**Table 1**). The 24-h sampling was performed before the daily 75 mg clopidogrel intake, whereas the 48-h sampling was afterward. All 30 enrolled patients were to be evaluated until 48 h after the loading dose; 9 patients did not undergo PCI because of unexpectedly mild stenosis and re-evaluation of the PCI indication on the following day and therefore, those patients discontinued clopidogrel intake. PCI was carried out in the remaining 21 patients and their blood samples were analyzed on days 14 (12–16) and 28 (26–30).

Analysis of Platelet Aggregation

Blood samples were collected using a 21G needle, with tourniquet, into a glass tube containing a final solution of 0.313% sodium citrate. Platelet-rich plasma (PRP) was prepared by centrifugation at 150 g at 25°C for 15 min and platelet-poor plasma was prepared by centrifugation at 1,740 g at 25°C for 10 min. The PRPs were stimulated by 5 and 20 μmol/L ADP (adenosine diphosphate; Chronolog), and 2 μg/ml collagen (Horm, Germany) at 37°C and the aggregations were analyzed, under stirring, using a 12-channel light transmission aggregometer (MCM HEMA TRACER 313; MC Medical, Japan), whereby the degree of light transmission of the PRP was defined as 0% of the aggregation rate and the cognitive platelet-poor plasma as 100%.[12,13] The degree of light transmission was monitored for 10 min after agonist stimulation and platelet aggregation was evaluated. All the procedures were completed within 2 h of blood sampling. The maximal aggregation rate (MAR) and the inhibition of platelet aggregation (IPA), which was calculated as the percent inhibition of baseline aggregation according to the following equation, were evaluated:

$$IPA(\%) = \{(MAR_{baseline} - MAR_{time\ after\ treatment})/MAR_{baseline}\} \times 100.$$

Table 1 Study Protocol

		Platelet function analysis
Day 0	*Clopidogrel 300 mg*	*1) Baseline* *2) 4 h after loading*
Day 1	*Clopidogrel 75 mg*	*3) 24 h after loading* *4) 48 h after loading*
Day 28	↓	*5) 14 days after loading* *6) 28 days after loading*

Analysis of Vasodilator-Stimulated Phosphoprotein (VASP) Phosphorylation

The VASP is an abundant substrate of cAMP-dependent protein kinase in platelets. Its phosphorylation levels were measured using the Platelet VASP-FCM kit (Biocytex Inc, Marseille, France) in which the VASP-phosphorylation levels are quantified by flow cytometry after stimulation of whole blood with prostaglandin E_1 (PGE_1; mean fluorescence intensity (MFI)) and also PGE_1 plus ADP (MFI PGE_1 + ADP). The $P2Y_{12}$ reactivity index (PRI), calculated as percent inhibition of baseline aggregation was evaluated according to the following equation:

$$PRI = \{(MFI_{PGE_1} - MFI_{PGE_1+ADP})/MFI_{PGE_1}\} \times 100.$$

Table 2 Baseline Characteristics

	Total (n=30)	*PCI (n=21)*	*Non-PCI (n=9)*	*P (PCI vs non-PCI)*
Age (years)	70±7	71±9	68±3	0.11
Males	22 (73%)	17 (81%)	5 (56%)	0.16
Platelets (×10⁴/μl)	21.1±5.5	20.4±5.2	22.2±5.8	0.43
Risk factors				
Current smoker	10 (33%)	11 (52%)	0 (0%)	0.0013
Hyperlipidemia[1]	22 (73%)	18 (86%)	5 (56%)	0.083
Diabetes[2]	7 (23%)	6 (29%)	1 (11%)	0.28
Hypertension[3]	18 (60%)	15 (71%)	4 (44%)	0.16
Prior myocardial infarction	1 (3%)	1 (5%)	0 (0%)	0.39
Prior PCI	4 (13%)	3 (14%)	1 (11%)	0.81
Prior cerebrovascular event	1 (3%)	1 (5%)	0 (0%)	0.39
Peripheral vascular disease	2 (7%)	2 (10%)	0 (0%)	0.22
Treatment				
β-blocker	4 (13%)	3 (14%)	1 (11%)	0.81
Nitrates	7 (23%)	5 (24%)	2 (22%)	0.92
ACEI/ARB	13 (43%)	8 (38%)	5 (56%)	0.38
Statin	26 (87%)	19 (90%)	7 (78%)	0.35
Ca-channel blocker	15 (50%)	12 (57%)	3 (30%)	0.23
Proton pump inhibitor	7 (23%)	5 (24%)	2 (22%)	0.92

Defined as [1]under medical treatment or total cholesterol level >220 mg/dl or low-density cholesterol level >140 mg/dl, [2]HbA1c >6.5%, [3]systolic blood pressure >140 mmHg or diastolic blood pressure >90 mmHg.
PCI, percutaneous coronary intervention; ACEI, angiotensin-converting enzyme inhibitor; ARB, angiotensin II-receptor blocker.

Table 3 Maximal Aggregation Rates (%)

	Baseline	4 h	24 h	48 h	14 days	28 days
ADP (5 μmol/L) stimulation						
Total (n=30)	64.5±6.7 (30)	53.8±10.1 (29)	52.9±8.9 (30)	49.0±10.2 (28)		
PCI-treated (n=21)	65.5±5.9 (21)	54.7±10.3 (20)	53.6±8.6 (21)	49.2±9.8 (20)	46.8±12.5 (20)	48.8±11.0 (21)
PCI-untreated (n=9)	62.0±8.2 (9)	52.0±10.0 (9)	52.0±10.0 (9)	48.6±11.8 (8)		
ADP (20 μmol/L) stimulation						
Total (n=30)	72.0±6.2	63.1±10.6	62.7±10.0	59.9±11.1 (28)		
PCI-treated (n=21)	72.8±6.5	63.8±10.7	62.7±9.6	60.1±11.4 (20)	55.8±10.2 (20)	57.0±10.3 (21)
PCI-untreated (n=9)	70.0±5.4	61.8±8.5	62.7±8.5	58.4±10.9 (8)		
Collagen (2 μmol/L) stimulation						
Total (n=30)	49.3±16.1	36.8±16.9	36.7±14.2	36.1±15.9 (28)		
PCI-treated (n=21)	50.3±15.8	40.1±16.8	38.3±13.2	37.7±14.2 (20)	33.1±12.2 (20)	34.8±11.9 (21)
PCI-untreated (n=9)	47.0±17.5	29.4±15.3	32.8±16.4	32.4±17.5 (8)		

Abbreviation see in Table 2.
The number of examined subjects is shown in parentheses.

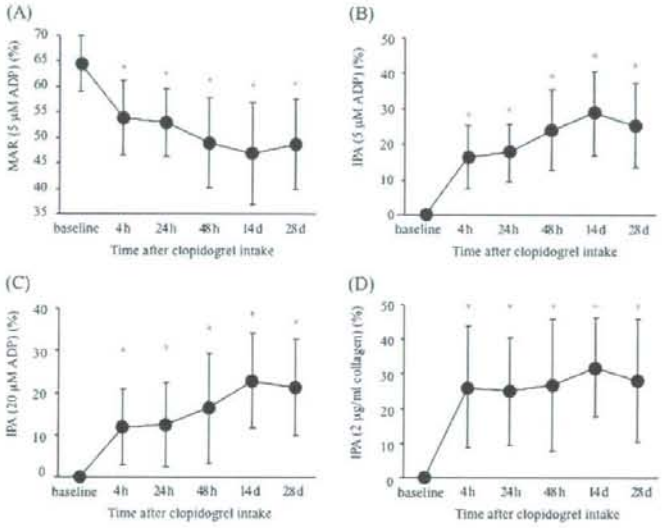

Fig 1. Time-dependent change in platelet aggregation after clopidogrel intake. (**A**) Maximal aggregation rates (MARs) induced with 5 μmol/L ADP. (**B**) Inhibition of platelet aggregations (IPAs) with 5 μmol/L ADP stimulation. (**C**) IPAs with 20 μmol/L ADP stimulation; (**D**) IPAs with 2 μg/ml collagen stimulation. By 1-sample t-test compared with the data at baseline, *P<0.0001.

Definition of Clopidogrel Responsiveness

Classification of clopidogrel effectiveness was based on the definition from a previous report:[14] IPA<10% (clopidogrel non-responders); 10%≤IPA<30% (hypo-responders); IPA≥30% (responders).

Statistic Analysis

Continuous variables are expressed as mean±SD. Categorical variables are expressed as frequencies and percentages. Comparisons between categorical variables were performed using 2-tailed Fisher's exact test or the Pearson's chi-square test. Student's t-test was used to compare continuous variables. Changes in parameters were analyzed using 1-sample t-test. A P-value <0.05 was defined as statistical significance. Statistical analyses were performed using StatView 5.0 software (SAS Institute, Cary, NC, USA).

Results

Characteristics of the Study Population

The baseline characteristics of the 30 enrolled patients are shown in **Table 2**. Mean age was 70±7 years and 22 patients (73%) were male. Only 1 patient (3%) had a history of prior myocardial infarction and 4 (13%) had undergone a prior PCI. Among the 30 patients, 9 did not undergo PCI because of unexpectedly mild stenosis on coronary angiography, which was not apparent on the initial non-invasive assessment. In the others (n=21), PCI with Cypher-stent® implantation was successfully performed. Blood examination was performed until 48 h after intake of 300 mg clopidogrel for all 30 patients, and additionally, on days 14 and 28 post-procedure for the 21 patients undergoing PCI. Because some patients did not cooperate, and other administrative reasons, a few data points were not available. The number of patients evaluated for platelet function was as follows: at 4 h (n=29), 24 h (n=30), and 48 h (n=28) after clopidogrel intake (n=30), and at 14 days (n=20) and 28 days (n=21) among patients undergoing PCI (n=21) (**Table 3**). In all 30 enrolled patients, we did not observe any haematologic disorders or liver dysfunction during the study period.

Baseline characteristics were not significantly different between the PCI (n=21) and non-PCI (n=9) groups, apart from smoking habit (**Table 2**). As shown in **Table 3**, there was no significant difference between the 2 groups in the